Available online at www.sciencedirect.com

ScienceDirect

www.journals.elsevier.com/jes

JES JOURNAL OF ENVIRONMENTAL SCIENCES

www.jesc.ac.cn

Preliminary investigation of phosphorus adsorption onto two types of iron oxide-organic matter complexes

Jinlong Yan[1], *Tao Jiang*[1,2,*], *Ying Yao*[3], *Song Lu*[1], *Qilei Wang*[1], *Shiqiang Wei*[1,*]

1. *Key Laboratory of Eco-environments in Three Gorges Reservoir Region, Ministry of Education, Chongqing Key Laboratory of Agricultural Resources and Environment, College of Resources and Environment, Department of Environmental Science and Engineering, Southwest University, Chongqing 400716, China. E-mail: yanjinlong6439@126.com*

2. *Department of Forest Ecology and Management, Swedish University of Agricultural Sciences, Umeå SE-90183, Sweden*

3. *School of Material Science & Engineering, Beijing Institute of Technology, Beijing 100081, China*

ARTICLE INFO

Article history:
Received 6 April 2015
Revised 24 August 2015
Accepted 27 August 2015
Available online 28 October 2015

Keywords:
Phosphorus
Ferrihydrite–humic acid complex
Goethite–humic acid complex
Adsorption

ABSTRACT

Iron oxide (FeO) coated by natural organic matter (NOM) is ubiquitous. The associations of minerals with organic matter (OM) significantly changes their surface properties and reactivity, and thus affect the environmental fate of pollutants, including nutrients (*e.g.*, phosphorus (P)). In this study, ferrihydrite/goethite-humic acid (FH/GE–HA) complexes were prepared and their adsorption characteristics on P at various pH and ionic strength were investigated. The results indicated that the FeO–OM complexes showed a decreased P adsorption capacity in comparison with bare FeO. The maximum adsorption capacity (Q_{max}) decreased in the order of FH (22.17 mg/g) > FH-HA (5.43 mg/g) > GE (4.67 mg/g) > GE-HA (3.27 mg/g). After coating with HA, the amorphous FH–HA complex still showed higher P adsorption than the crystalline GE–HA complex. The decreased P adsorption observed might be attributed to changes of the FeO surface charges caused by OM association. The dependence of P adsorption on the specific surface area of adsorbents suggests that the FeO component in the complexes is still the main contributor for the adsorption surfaces. The P adsorptions on FeO–HA complexes decreased with increasing initial pH or decreasing initial ionic strength. A strong dependence of P adsorption on ionic strength and pH may demonstrate that outer-sphere complexes between the OM component on the surface and P possibly coexist with inner-sphere surface complexes between the FeO component and P. Therefore, previous over-emphasis on the contributions of original minerals to P immobilization possibly over-estimates the P loading capacity of soils, especially in humic-rich areas.

Introduction

The phosphorus (P) cycle in the environment is an important biogeochemical process which could strongly influence agricultural nonpoint source pollution, soil fertility, soil erosion, and water eutrophication, *etc.* Thus, the fate, transport, and transformation of P in the environment have attracted tremendous attention (Ekholm and Lehtoranta, 2012; Lijklema, 1980; Sharpley et al., 1994). As a key factor to control P cycling, especially in redox-changing environments such as wetlands, water-level fluctuation zones and riparian areas, iron oxide (FeO) (*e.g.*, goethite (GE) and ferrihydrite (FH)) plays an important role in P immobilization and release due to its large surface area, variable-charge surface and high reactivity.

* *Corresponding authors.* E-mail: jiangtower666@163.com (Tao Jiang), sqwei@swu.edu.cn (Shiqiang Wei).

http://dx.doi.org/10.1016/j.jes.2015.08.008
1001-0742/

The amount of P adsorbed by the soil has a linear relationship with the amorphous and crystalline FeO contents of the soil (Axt and Walbridge, 1999; Zhang et al., 2003). However, FeO rarely occur alone in the environment; they often are associated with natural organic matter (NOM) including humic substances to form FeO–organic matter (OM) complexes (Fontes et al., 1992; Schwertmann et al., 2005; Weng et al., 2006a), which are an important component of soil aggregates and have a significant effect on soil properties (Xiong and Li, 1987). Physical adsorption, ligand exchange, protonation, hydrogen bonding, and cation bridging are main mechanisms responsible for the interaction between OM and FeO (Gu et al., 1994). In addition, FeO–OM complexes are also important for the stabilization of OM in soil (Baldock and Skjemstad, 2000; Kaiser and Guggenberger, 2000) as they inhibit the biodegradation of OM and extend the turnover time. The complexes also serve as a crucial mechanism for carbon sequestration (Baldock and Skjemstad, 2000; Kalbitz et al., 2005), thereby affecting the global carbon cycle. In addition, NOM can inhibit the crystallization of amorphous FeO due to the formation of iron mineral–OM complexes (Schwertmann, 1966). Because of mineral-bound OM, mineral transformation during abiotic or biotic reduction is clearly changed (Henneberry et al., 2012; Shimizu et al., 2013).

Such changes of iron minerals also strongly affect the cycling of iron, consequently influencing the adsorption capacity of minerals for pollutants including oxyanions such as PO_4^{3-} (Gerke and Hermann, 1992; Laor et al., 1998; Vermeer et al., 1999). Thus, gaining further understanding of the details and mechanisms of P adsorption by FeO–OM complexes could be helpful in unraveling the processes of retention, bioavailability and bioaccumulation of P in natural ecosystems. Although FeO–OM complexes play a significant role on the chemical behavior of environmental pollutants, studies regarding their effects on the transport and transformation of P are still insufficient. Previously, most studies only focused on the competitive adsorption of OM and P onto raw FeO surfaces (Borggaard et al., 2005; Geelhoed et al., 1998; Hiemstra et al., 2013; Weng et al., 2008), while the interactions between P and FeO–OM complexes, which could be ubiquitous geochemical process occurring in environments such as sediments and wetlands, remain unknown.

The main objectives of this study were to find out whether mineral-bound OM promotes or reduces P sorption, and provide more details about the changes of P sorption capacity. Effects of pH and iron strength were also investigated. We believe that the findings here would be useful and pertinent to exploration of the underlying mechanism controlling P release from soils/sediments, and the relationship between P and mineral-OM for further understanding of eutrophication and OM stabilization, especially in the context of global climate change.

1. Materials and methods

1.1. *Preparation and characterization of FeO–HA complexes*

Millipore® ultrapure (18.2 MΩ· cm) water was used, and all chemical reagents were of ultrapure grade. Preparation of pure FeO was carried out based on the method reported by Schwertmann and Cornell (2000). The detailed procedures were as follows. For FH preparation: 40 g $Fe(NO_3)_3{\cdot}9H_2O$ was weighed and added to 500 mL of deionized (DI) water. Then, 330 mL of 1 mol/L KOH was added under vigorous stirring using a magnetic stirrer; the final 20 mL was added dropwise to adjust the pH to 7.5. After the pH was adjusted, the mixture was stirred for 30 min and centrifuged at 4000 r/min for 10 min. Washing with DI water was carried out several times until the conductivity of the eluate was less than 50 μS/cm. After freeze-drying, the sample was ground in an agate mortar, passed through a 100-mesh sieve, and stored in a refrigerator at 4°C. Thus, the FH solid was obtained. For GE preparation: 50 mL of 1 mol/L $Fe(NO_3)_3$ solution was transferred to a 1 L polyethylene bottle. Then, 90 mL of a 5 mol/L KOH solution was added rapidly under vigorous stirring using a magnetic stirrer. Water was added to adjust the final volume to 1 L and the mixture was then sealed using a polyethylene film; the initial pH of the suspension was 12. After storage at 70°C for 60 hr, the mixture was centrifuged at 4000 r/min for 10 min. The subsequent steps were the same as for FH preparation.

Preparation of FeO–OM complexes was carried out according to the method reported by previous researchers with modification (Cruz-Guzmán et al., 2003; Sharma et al., 2010). We used humic acid (HA) to represent OM. The detailed procedures were as follows. According to the method for preparing pure FeO (as above-mentioned), the wet FH (or GE) was transferred to a 1 L beaker. Then, 500 mL (or 250 mL) of deionized water was added to obtain a suspension of FeO, followed by the addition of 2 g (or 1 g) of HA (>90% HA, Adamas, purchased from Tansuo Co. Ltd., China). No further purification of HA was conducted. The basic properties of HA were as follows: The Brunauer–Emmett–Teller (BET) specific surface area (SSA) 4.36 m^2/g; C 39%; N 1%; H 3%. The initial C/Fe mass ratio of the prepared complex in solution was 0.015. The initial pH of FH-HA as-prepared was 8.3, and the initial pH of GE-HA as-prepared was 9.5. The mixture was stirred for 24 hr in the dark, aged for 12 hr, and centrifuged at 4000 r/min for 30 min. The subsequent steps were the same as for pure FeO preparation. Finally, the carbon contents in the FH–HA and GE–HA complexes were 7.12% and 1.32%, respectively.

Characterization of FeO–HA complexes and pure FeO: X-ray diffraction (XRD) patterns were obtained using a X-ray diffractometer (Beijing Purkinje General XD-3, China) and the detailed operation conditions were as follows: anode material: Cu target; tube voltage: 36 kV; tube current: 20 mA; scanning speed: 2°/min; step size: 0.04° (2θ); slit (FS-FSS-JS): 1°–0.3°–1°; scan angle: 10–70° (2θ); graphite monochromator. Scanning electron microscopy (SEM) analysis was performed using an electron microscope (JEOL JSM-6510LV, Japan) with an accelerating voltage of 20 kV. Fourier transform infrared spectroscopy (FT-IR) analysis was conducted using an infrared spectrometer (Thermo Scientific Nicolet iS10, USA) with a scan range of 400–4000 cm^{-1}. The BET SSA was determined using nitrogen adsorption–desorption (Micromeritics ASAP 2020V4.00, USA). The point of zero charge (PZC) was determined through acid-base titrations (702 SM Titrino, Metrohm, Switzerland) (Wei and Xiang, 2013; Wei et al., 2014). The carbon content in the FeO–HA complexes was determined by an Infrared Sulfur and Carbon Analyzer-HCS878G (Sichuan Jingke Instrument Manufacturing Co. Ltd., China).

1.2. Adsorption kinetics

0.040 g samples of the FeO–HA complexes were prepared, with the addition of 25 mL of a 20 mg/L KH_2PO_4 solution (P concentration), in 100 mL centrifuge tubes. The pH and solution ionic strength (I) of the system were controlled at 7 and 0.01 mol/L KNO_3, respectively. Samples oscillating at a constant temperature (25°C) and rotation speed (220 r/min), for 1, 5, 10, 20, 30, 60, 180, 720, 1080, 1440, 2160, and 2880 min were filtered through a mixed cellulose ester 0.45 μm filter membrane to determine the P content in the filtrate. P content was determined using the modified molybdenum blue method (Murphy and Riley, 1962; Wei, 2002), with pure FeO as the control (the same method is used for determining P concentration in subsequent sections).

1.3. Adsorption isotherms

0.040 g samples of the FeO–HA complexes were prepared, with the addition of 25 mL of 1, 5, 10, 15, 20, 50, 80, 120, 180, and 250 mg/L KH_2PO_4 solutions (P concentration), in 100 mL centrifuge tubes. The pH and I of the system were controlled at 7 and 0.01 mol/L KNO_3, respectively. After oscillating at a constant temperature (25°C) and rotation speed (220 r/min) for 24 hr, the samples were filtered through a 0.45 μm membrane to determine the P concentration in the filtrate.

1.4. Effects of ionic strength on adsorption

0.040 g samples of the FeO–HA complexes were prepared, with the addition of 20 mg/L KH_2PO_4 solution (P concentration), in 100 mL centrifuge tubes. The I values of the system were controlled at 1, 0.1, 0.01, and 0.001 mol/L KNO_3, while the pH was adjusted to 7. After oscillating at a constant temperature (25°C) and rotation speed (220 r/min) for 24 hr, the samples were filtered through a 0.45 μm membrane to determine the P concentration in the filtrate.

1.5. Effects of pH on adsorption

0.040 g samples of the FeO–HA complexes were prepared, with the addition of 20 mg/L KH_2PO_4 solution (P concentration), in 100 mL centrifuge tubes. The pH values of the system were controlled at 2, 3, 5, 7, 9, 11, and 12, while the I value was maintained at 0.01 mol/L KNO_3. After oscillating at a constant temperature (25°C) and rotation speed (220 r/min) for 24 hr, the samples were filtered through a 0.45 μm membrane to determine the P concentration in the filtrate.

1.6. Data processing

Triplicate measurements of the samples, blank control group (P-free), and adsorption-agent-free control group were conducted for each adsorption experiment. All results are reported here as average values and the relative standard deviation was less than 5%. Data processing and plotting were carried out using Origin 8.5 and Excel 2013.

2. Results and discussion

2.1. Structural features of FeO–HA complexes

The XRD patterns showed that synthesized pure FH and GE exhibited the specific peaks well-matched well with those of standards, which indicated that the prepared FH had poor crystallinity with a 2-line pattern and the prepared GE had good crystallinity (Fig. 1). In contrast, both types of FeO–HA complexes showed lower intensity diffraction peaks compared with pure FeO; for instance the peaks of the GE-HA complex corresponding to the 101, 040, and 041 crystal planes almost disappeared, and the peaks of the FH–HA complex at 0.250 nm and 0.151 nm became broad, revealing poorer crystallinity.

FH particles had an irregular shape, with some small holes and wrinkles on an uneven surface, with BET SSA of 259.8 m^2/g (Fig. 2a). For FH–HA, HA particles were tightly bound to the FH surface, and some particles entered the holes and wrinkles on the FH surface, and the BET surface area decreased to 163.3 m^2/g (Fig. 2b). The GE particles showed an obvious acicular-shaped morphology with non-uniform diameter, smooth surface, and SSA of 31.7 m^2/g (Fig. 2c). The GE–HA particles had uniform morphology and showed significant agglomeration due to the wrapping of flaky particles with acicular particles. The agglomerated particles had non-uniform size and the SSA was reduced to 25.5 m^2/g (Fig. 2d). Clearly, this reveals that the coating of HA can decrease the surface area of iron minerals, which is in line with the observation of Kaiser and Guggenberger (2003) that sorption of OM reduced the mineral SSA.

The FT-IR spectra of FeO–HA complexes and pure FeO are shown in Fig. 3. The peaks of pure FeO at 464, 561, 1028 cm^{-1} and 634, 797, 892 cm^{-1} were the characteristic absorption peaks for FH (Mazzetti and Thistlethwaite, 2002; Musić et al., 1993) and GE (Xu et al., 2013), respectively. Meanwhile, both FH–HA and GE–HA also showed the above-mentioned peaks consistent with the corresponding pure FeO. These results indicate that the combination of HA and FeO did not change the internal structure of the FeO, which is consistent with the results of XRD. For FH–HA, the peak at 1385 cm^{-1} caused by residual NO_3^- during FH preparation (Mazzetti and Thistlethwaite, 2002) was significantly lower than that of FH, which may be due to the fact that the NO_3^- adsorbed on the FeO surface was replaced by HA. Compared with FH, the absorption peaks of FH-HA at about 3400 cm^{-1} were red-shifted with a decrease in peak intensity; the peak intensity at 1618 cm^{-1} was reduced and the peak was broadened; in addition, an absorption peak appeared at 1561 cm^{-1}, and both two peaks corresponded to the –OH group (Mazzetti and Thistlethwaite, 2002; Russell, 1979). Meanwhile, similar results were obtained for both GE–HA and GE (Xu et al., 2013). The above peak changes in the FeO–HA acid complexes at 3400 and 1600 cm^{-1} may be caused by the binding of HA onto FeO. In addition, compared with HA, the symmetric stretching vibration peak of COO^- groups at 1389 cm^{-1} disappeared in FeO–HA complexes, and the intensity of the antisymmetric stretching peak of COO^- groups at 1618 cm^{-1} declined or disappeared (Hay and Myneni, 2007).

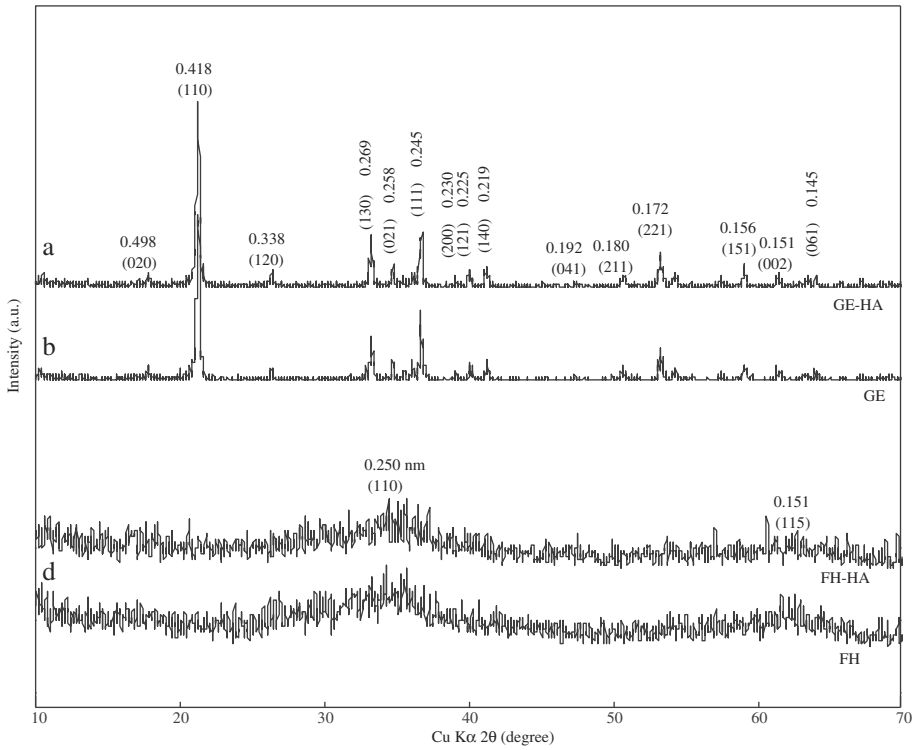

Fig. 1 – X-ray diffraction (XRD) patterns with Cu-Kα radiation of freeze-dried samples including: (line a) goethite-humic acid, (line b) goethite, (line c) ferrihydrite-humic acid, (line d) ferrihydrite.

Therefore, these results clearly suggested that FeO–HA complexes were formed by ligand exchange between the –OH on the surface of FeO and the – COOH of HA (Leone et al., 2001; Sharma et al., 2010; Weng et al., 2006b).

2.2. Adsorption kinetics

The adsorption kinetics of P on FH–HA and GE–HA can be divided into rapid and slow adsorption phases (Fig. 4), which are 0–60 min and 60–2880 min for FH–HA, and 0–30 min and 30–2880 min for GE–HA, respectively. The reaction process was similar to that of P adsorption on pure FeO reported before (Arai and Sparks, 2007; Wang et al., 2013a). Generally speaking, except for FH, the other three minerals reached adsorption equilibrium within approximately 24 hr. The fitting of experimental data was conducted using the Elovich, exponential, parabolic, intraparticle diffusion, and pseudo-first order kinetics equations. It was found that a pseudo-first order kinetics equation provided a good fit for P adsorption during the whole adsorption process, including rapid and slow phases, with the highest r^2 values. The fitting parameters are shown in Table 1, and the kinetics equation is $\mathrm{Ln}(C_0/C) = kt + b$, where C_0 (mg/L) is the initial P concentration, C (mg/L) is the concentration of P in solution at time t, k (min^{-1}) is the pseudo-first order rate constant, and b is a constant (Wang et al., 2013b). The values of the rate constant during the rapid adsorption phase (k_{rap}) varied in the order: 8.1×10^{-3} min^{-1} (FH) > 2.1×10^{-3} min^{-1} (GE) > 9.4×10^{-4} min^{-1} (FH–HA) > 9.2×10^{-4} min^{-1} (GE–HA). The values of the rate constant during the slow adsorption phase (k_{slow}) were in the order: 4.11×10^{-4} min^{-1} (FH) > 6.38×10^{-5} min^{-1} (FH-HA) > 2.55×10^{-5} min^{-1} (GE-HA) > 1.46×10^{-5} min^{-1} (GE). By the end of adsorption process, the amounts of P adsorbed by FH–HA and GE–HA during the rapid adsorption stage only accounted for 29.13% and 54.04% of the total adsorption, respectively, while those of FH and GE accounted for 61.27% and 85.93%, respectively. Clearly, the combination of HA with FeO caused the decrease of P sorption during the rapid phase but increased it during the slow stage for FeO–HA complexes compared with

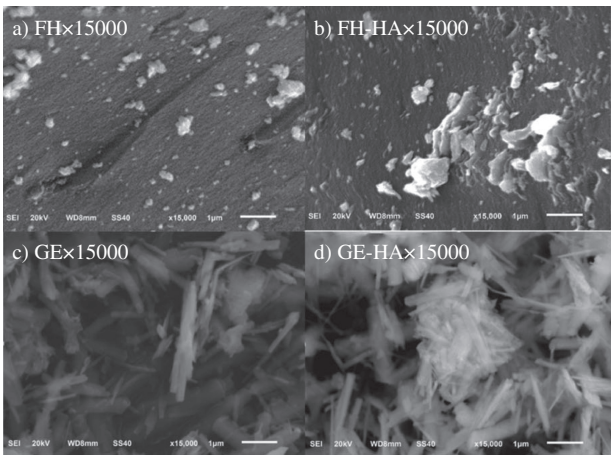

Fig. 2 – Scanning electron microscope (SEM) images of iron oxide-humic acid complexes. (a) ferrihydrite, (b) ferrihydrite-humic acid, (c) goethite, (d) goethite-humic acid.

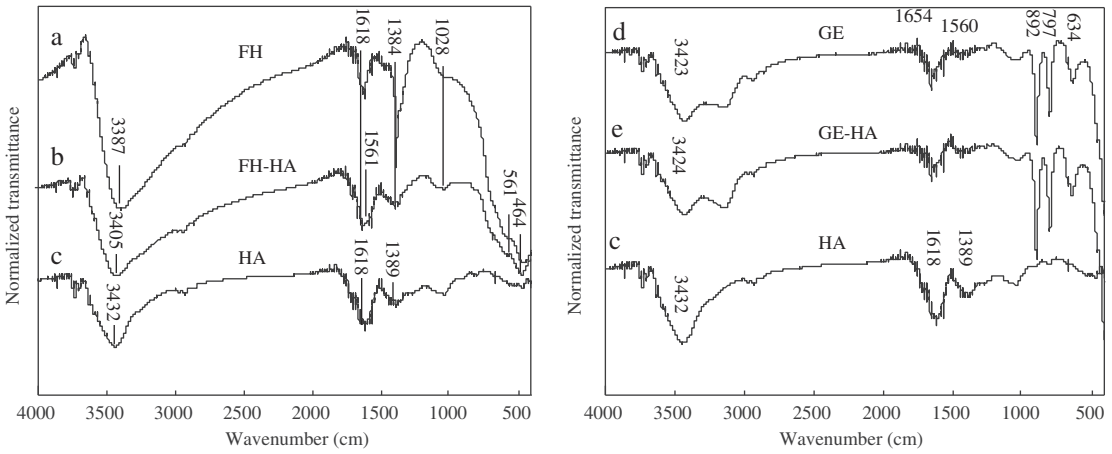

Fig. 3 – Fourier transform infrared spectroscopy (FT-IR) spectra of freeze-dried samples. Labels correspond to different samples: (line a) ferrihydrite, (line b) ferrihydrite-humic acid, (line c) humic acid, (line d) goethite, and (line e) goethite-humic acid. Spectra baselines were offset to improve visual clarity of FT-IR spectra.

amorphous FeO alone. GE is a crystalline iron mineral with a relatively small amount of adsorption sites, as compared with amorphous FH with a large SSA and adsorption sites available. Thus GE could rapidly reach adsorption saturation during the rapid adsorption phase, and the adsorption rate was significantly reduced during the slow adsorption phase. Meanwhile, the advent of equilibrium for the adsorption of P on GE–HA was delayed because of inhibition by HA, and the rate constant of GE–HA was higher than GE at the slow P adsorption stage. On the other hand, the latter had sufficient adsorption sites and the highest SSA value, resulting in diffusion behavior that lasted for a longer time, and the adsorption rate constant was higher than FH–HA during both rapid and slow phases.

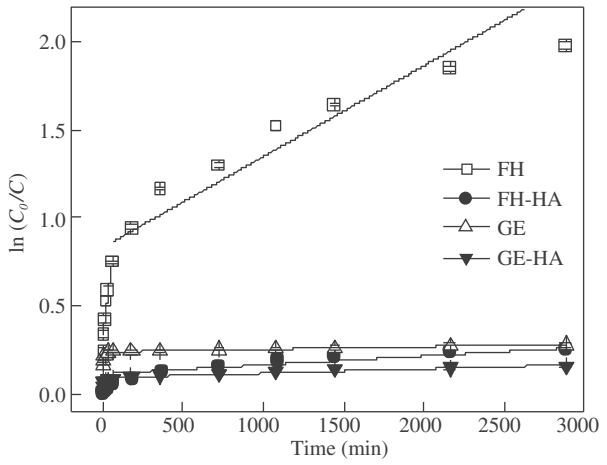

Fig. 4 – Pseudo-first order kinetics fitting curves for two stages of phosphorus adsorption on iron oxide-humic acid complexes with an initial phosphorus concentration of 20 mg/L (pH 7.0, 0.01 mol/L KNO_3). FH: ferrihydrite, GE: goethite, HA: humic acid; FH-HA: ferrihydrite-humic acid; GE-HA: goethite-humic acid.

2.3. Adsorption isotherms

As shown in Fig. 5, the amount of P adsorbed on FeO–HA complexes increased with the initial P concentration, which is similar to the result on pure FeO. When the initial P concentration was less than 50 mg/L, the amount of adsorbed P increased rapidly. However, the amount of adsorbed P increased much more slowly when the concentration was greater than 50 mg/L. The Langmuir (Eq. (1)) and Freundlich (Eq. (2)) isotherm models, were used to fit the data.

$$Q_e = Q_{max} \times k_L \times C_e/(1 + k_L \times C_e) \quad (1)$$

$$Q_e = k_F \times C_e^{1/n} \quad (2)$$

where, Q_e (mg/g) is the amount of adsorbed P, Q_{max} (mg/g) is the maximum adsorption capacity, and k_L, k_F, and n are all constants related to the adsorption. Results showed that both provided a good fit for P isothermal adsorption.

According to the Langmuir fitting results, the Q_{max} values (expressed on a mass basis) varied in the following order: 22.17 mg/g (FH) > 5.43 mg/g (FH–HA) > 4.67 mg/g (GE) > 3.27 mg/g (GE–HA) (Table 2). By comparing the Gibbs free energy (ΔG) and adsorption equilibrium parameter (R_L),

Table 1 – Fitting results of the pseudo-first order kinetics equation for two stages of phosphorus adsorption on iron oxide-humic acid complexes. The whole kinetics process was divided into two parts including rapid and slow stages.

	$Ln(C_0/C) = kt + b$					
	k_{rap} (min^{-1})	b_{rap}	r^2_{rap}	k_{slow} (min^{-1})	b_{slow}	r^2_{slow}
FH	8.06×10^{-3}	0.31	0.90	4.11×10^{-4}	0.94	0.90
FH-HA	9.38×10^{-4}	0.014	0.85	6.38×10^{-5}	0.097	0.85
GE	2.08×10^{-3}	0.18	0.84	1.46×10^{-5}	0.24	0.99
GE-HA	9.21×10^{-4}	0.056	0.64	2.55×10^{-5}	0.091	0.88

FH: ferrihydrite; GE: goethite; HA: humic acid; FH-HA: ferrihydrite-humic acid; GE-HA: goethite-humic acid.

it could be concluded that the FeO–HA complexes significantly decreased the P adsorption ability. R_L was less than 1 in all cases, which revealed that the adsorption processes were favorable. However, the R_L of the complexes were closer to 1, indicating that P adsorption on complexes appeared less favorable than on the raw iron minerals. In addition, it could be observed in Table 2 that the original iron minerals had greater maximum buffer capacity (MBC) than the complexes. This suggestted that the adsorption capacity of P on the complexes decreased, which was also demonstrated by Freundlich modeling.

The value of 1/*n* in the Freundlich model reflects the adsorption strength (Stellacci et al., 2009); the smaller the value, the more preferential the adsorption properties. A value of 1/*n* close to 0 suggests the adsorption surface is more heterogeneous (Sposito, 1989; Lu et al., 2014). Usually, a material with a 1/n value of 0.1–0.5 has a high adsorption capacity. In this study, the 1/*n* values for P adsorption onto the four materials varied in the following order: 0.21 (FH) < 0.27 (GE) < 0.33 (FH-HA) < 0.43 (GE-HA). This suggestted that the raw FeO had higher heterogeneity than the organic-mineral complexes. This conclusion was supported by the observed morphologies in SEM images and the reduced SSA after HA coating.

Additionally, both the k_L and k_F values in the two models reflect the binding constants (Borggaard et al., 2005). The k_L and k_F values of FH–HA and GE–HA were far less than those of FH and GE, demonstrating that the P binding capacities of the FeO–HA complexes were much lower than those of raw iron minerals. Besides, the reduction degree of P adsorption onto the iron mineral-HA complexes clearly depended on the type of mineral. Amorphous FeO (FH) associated with HA still showed higher reactivity in comparison with the relatively crystalline FeO–HA (GE–HA) complex.

Table 2 – Adsorption model fitting results for the phosphorus adsorption isotherms of the iron oxide-humic acid complexes.

	FH	FH-HA	GE	GE-HA
Langmuir fitting				
k_L	0.17	0.05	0.13	0.05
Q_{max} (mg/g)	22.17	5.43	4.67	3.27
Q_{max} (mg/m^2)	0.085	0.033	0.147	0.128
MBC[a](mg/g)	3.77	0.29	0.61	0.17
ΔG[b](kJ/mol)	−21.24	−18.35	−20.58	−18.31
R_L[c]	0.85	0.95	0.88	0.95
r^2	0.99	0.99	0.99	0.95
Freundlich fitting				
k_F	7.52	0.90	1.29	0.40
n	4.87	3.05	3.73	2.35
r^2	0.99	0.99	0.98	0.94

FH: ferrihydrite; GE: goethite; HA: humic acid; FH-HA: ferrihydrite-humic acid; GE-HA: goethite-humic acid.

[a] MBC is the maximum buffer capacity of adsorption. MBC = $k_L \times Q_{max}$. Higher MBC means greater adsorption capacity of adsorbent.

[b] ΔG is the adsorption reaction Gibbs free energy. $\Delta G = -R \times T \times \mathrm{Ln}(k_L \times 30974)$, R = 8.314 J/mol, T = 298.15 K (25°C). More negative value means the adsorption can occur more spontaneously.

[c] R_L is a dimensionless constant called the adsorption equilibrium parameter, which is defined as $R_L = 1/(1 + k_L \times C_0)$. C_0 (mg/L) is the initial concentration. Adsorption process is indicated by either unfavorable ($R_L > 1$), linear ($R_L = 1$), favorable ($0 < R_L < 1$) or irreversible ($R_L = 0$).

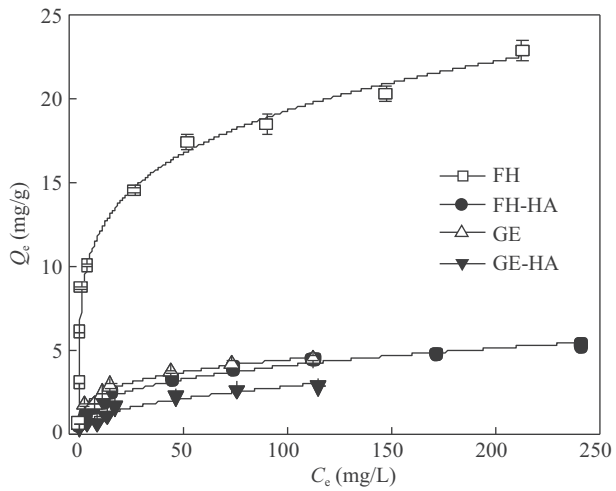

Fig. 5 – Adsorption isotherms of phosphorus on the iron oxide-humic acid complexes with the Freundlich model at pH 7.0 and 0.01 mol/L KNO_3 after 24 hr equilibrium time. The data points represent the adsorption amount of P (Q_e) at a relevant equilibrium concentration of solution (C_e), FH: ferrihydrite; GE: goethite; HA: humic acid; FH-HA: ferrihydrite-humic acid; GE-HA: goethite-humic acid.

Further, the different SSA of the minerals may also explain the different P adsorption results onto the four adsorbents, because SSA can provide an estimation of the potential available sites for P sorption. We also observed a similar positive relationship between the SSA of adsorbents and the Q_{max} of P sorption as reported by Nelson et al. (1992), indicating that the Q_{max} depended on minerals SSA by a certain degree. Thus, the SSA of raw FeO was larger compared to FeO–HA complexes, which showed that P-mineral interactions on the former surfaces were higher than on the latter surfaces. When Q_{max} is expressed as mg/m^2 derived from SSA, as shown in Table 2, the order of increasing sorption, GE > GE-HA > FH > FH-HA, is different from the order when Q_{max} is expressed on a mass basis (FH > FH-HA > GE > GE-HA). This Q_{max} (mg/m^2) order might also reflect a possibly increasing trend of mineral surface area charge density, and therefore evidentially support the hypothesis that changes of surface charge possibly play an important role in the processes. Considering the surface charge of adsorbents, FeO including FH and GE usually have a higher point zero of charge (PZC) than HA (PZC of FH at pH 7.9, PZC of GE at pH 7.5–9.5, but PZC of HA at pH 2–4) (Kleber et al., 2015; Qin et al., 2015). Thus the PZC of the complexes should be between the PZC of raw iron mineral and HA. In fact, we measured the PZC of the four adsorbents in this study. The results were consistent with the above analysis: the PZC of FH,FH-HA,GE and GE-HA were 8.2,7.7, 9.1 and 8.5, respectively. At pH = 7 in this isothermal experiment, the FeO surface becomes more negative after HA coating. So, the surface

of minerals dominated by HA in FeO–HA complexes was inclined to restrain rather than increase P adsorption.

Thus, according to the aforementioned experimental results and explanations, we could speculate that the possible reasons for decreasing P adsorption on FeO-HA were three-fold: (1) the main adsorption surface was that of the iron mineral rather than HA. Interaction between P and the iron mineral still controls the final P adsorption that we observe; (2) HA coating is inclined to act as a competitor with P to occupy the binding sites on the mineral surface, resulting in further reduction in P adsorption. The main coordinating groups on the surface of FeO were $FeOH^{1/2-}$, Fe_2OH^0, $Fe_3O^{1/2-}$. However, Fe_2OH^0 groups are inert in the near-neutral pH range, and the reactions between $Fe_2OH^0/Fe_3O^{1/2-}$ groups and phosphate can often be ignored (Antelo et al., 2005, 2010; Tadanier and Eick, 2002). So, $FeOH^{1/2-}$ on the FeO surface may be the adsorption sites occupied by the HA coating in our study. P could be bound to HA *via* metal bridges such as with organically complexed Fe^{3+} (Gerke and Hermann, 1992), although this contribution is also negligible; and (3) the more negative surface charge resulting from the HA coating repulses further P adsorption.

2.4. Effects of ionic strength

The effects of different initial concentrations of electrolyte (KNO_3) on P adsorption on FeO–HA complexes were investigated when the initial P concentration was 20 mg/L and pH was 7 (Fig. 6). With increasing initial KNO_3 concentration, the amounts of adsorbed P on the four minerals all gradually increased. For P adsorption on FH-HA and GE-HA, both showed similar trends as on the raw iron minerals. Some studies found (Antelo et al., 2005; Rahnemaie et al., 2007) that at relatively low pH, the increase in electrolyte concentration had less impact on P adsorption; while when pH was greater than 6 the increase in electrolyte concentration favored P adsorption. This could be explained by high electrolyte concentration changing the surface potential of adsorbent and reducing electrostatic repulsion, which promotes P adsorption (Rahnemaie et al., 2007). More importantly, the cation K^+ may bridge the negatively charged surfaces of solid mineral phases and negatively charged PO_4^{3-} (Arai and Sparks, 2001). Additionally, the influence of ionic strength on P adsorption on FeO–HA complexes is more sensitive for the amorphous FH–HA complex than the crystalline GE–HA complex. We calculated the net increase of P sorption (P_{net}) due to increasing K^+ from 0.001 to 1 mol/L; the difference for FH (2.21 mg/g) was more significant than for FH-HA (1.52 mg/g), which was greater than the difference observed between GE (1.09 mg/g) and GE-HA (1.14 mg/g). The role of the cationic bridge may be masked because of the obvious differences in adsorption capacity; as a result, the increase in P adsorption for FH-HA was lower than that for FH, while the increase for GE-HA was slightly higher than that for GE.

Further, a strong dependence on ionic strength is typical for outer-sphere rather than inner-sphere complexation. However, at high electrolyte concentrations, P adsorption on FeO still leads to an increase in the formation of inner-sphere complexes, whose negative surface charge is neutralized by the co-adsorbed electrolyte cations (*e.g.*, K^+, Na^+), thereby promoting P adsorption (Arai and Sparks, 2001) with increasing *I*. The reaction is as follows:

$$\equiv Fe\text{-}OH + K^+ + HPO_4^{2-} \rightarrow \equiv Fe\text{-}O\text{-}PO_3H\cdots K^+ + H_2O.$$

Thus, this observation seems to indicate that for P adsorption on FeO–HA complexes, outer-sphere complexes between the OM component surface and P involving electrostatic bonding mechanisms possibly coexist with inner-sphere surface complexes between the iron mineral component and P, which necessarily involve largely covalent bonding.

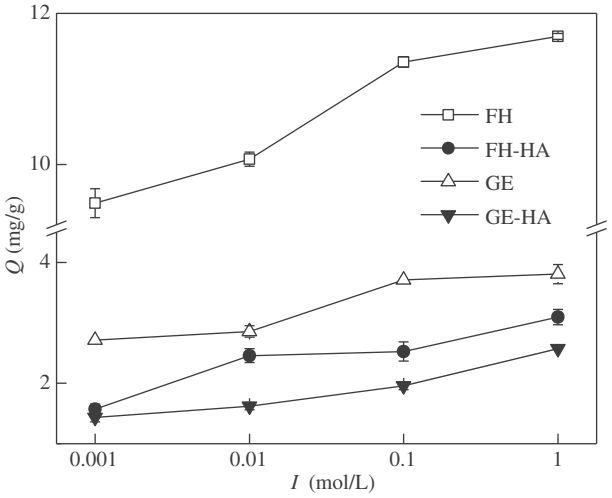

Fig. 6 – Phosphorus adsorption changes of iron oxide-humic acid complexes at different electrolyte concentrations with an initial phosphorus concentration of 20 mg/L (pH 7.0) after 24 hr equilibration time. The data points represent the adsorption amount of P (Q) at a given electrolyte concentration (*I*), FH: ferrihydrite; GE: goethite; HA: humic acid; FH-HA: ferrihydrite-humic acid; GE-HA: goethite-humic acid.

2.5. Effects of pH

The effects of initial pH (2–12) on the P adsorption on FeO–OM complexes were explored with the initial P concentration of 20 mg/L and *I* of 0.01 mol/L (Fig. 7). In our study, pH dependency of P adsorption was observed in all four minerals. It was found that the amount of adsorbed P on FH-HA and GE-HA decreased with increasing initial pH values, which was consistent with the trends in raw FeO as reported previously (Geelhoed et al., 1997), and also similar to previous reports on sorption of other oxyanions (*e.g.*, arsenate) (Xie, 2012). After HA is coated on a mineral, due to the PZC decrease, the surface becomes more negatively charged due to surface deprotonation from increasing pH, so PO_4^{3-} adsorption becomes less electrostatically favorable. In particular, this may occur for the reduction in P adsorption at high pH (Antelo et al., 2010), such as was the case at pH = 12 in our study. Additionally, there were no significant differences in pH impact between FeO–HA complexes and pure FeO. HA coating possibly changed the surface PZC of iron minerals, but did not change the adsorption mechanism of P on the solid phase.

The pH-dependent adsorption might be a strong piece of evidence to support that iron mineral controls the P adsorption. Comparatively, pH increase leads to increase of P adsorption in the case of P binding with HA *via* iron bridging (Gerke and Hermann, 1992), thus the results in our study also indicate that interaction between P and HA could not be the main mechanism for P adsorption by FeO–HA complexes.

2.6. Comparison and environmental implications

In this study, the mineral phase was the key factor in the process of P adsorption on FeO–HA complexes, rather than the organic phase. HA in the complexes occupies a large number of adsorption sites on the mineral surface, but this did not change the tendency of P adsorption, which was not consistent with the mechanisms from previous studies on the adsorption of heavy metals or organic pollutants by FeO–OM complexes (Table 3). Previous studies showed that both FeO and OMs in FeO–OM complexes are almost equally responsible for adsorption of heavy metals or organic pollutants. OM loaded on minerals could even provide extra sites available for metal ion binding, and increase the hydrophobicity to promote the "hydrophobic interaction" with organic pollutants. In contrast, in terms of the effect on P adsorption, the result was similar that of arsenic adsorption as previously reported (Ko et al., 2004; Xie, 2012), as arsenate and phosphate are both oxyanions sharing similar geochemical properties.

We believe that the P bound to FeO–HA complexes also has profound environmental implications, as mineral-OM associations are ubiquitous in the environment. Under certain favorable conditions, the complexes may also become mobilized and transported in dissolved and colloidal forms, thus increasing P mobility. Additionally, currently ternary complex formation between arsenate and Fe^{3+}-OM co-precipitation has been proposed to explain the role of iron-OM in arsenate adsorption and mobility. However, further investigation is needed to understand whether this mechanism for P binding occurs in bulk OM coated on FeO, because releases of Fe^{3+}/Fe^{2+} from solid mineral phases is ubiquitous in wetlands, flooded soils and sediments under anoxic conditions (Elsner et al., 2004).

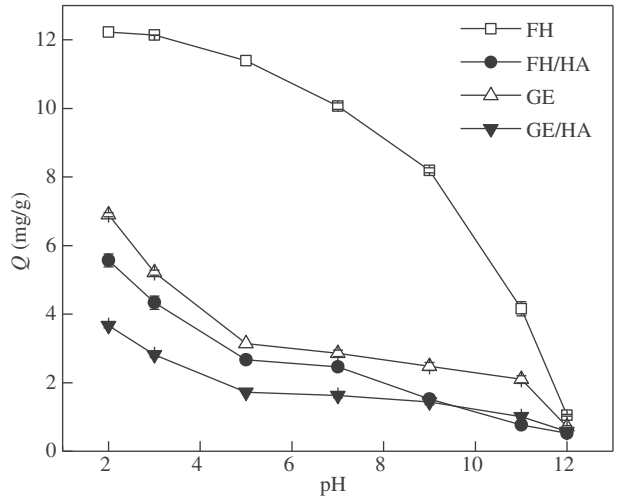

Fig. 7 – Phosphorus adsorption changes of iron oxide-humic acid complexes at different pH conditions with an initial phosphorus concentration of 20 mg/L (I = 0.01 mol/L KNO_3) after 24 hr equilibrium time. The data points represent the adsorption amount of P (Q) at a given pH value, FH: ferrihydrite; GE: goethite; HA: humic acid; FH-HA: ferrihydrite-humic acid; GE-HA: goethite-humic acid.

FeO in the environment are often associated with NOM, with more than 20% of OM being buried in sediments bound to iron mineral surfaces (Lalonde et al., 2012). However, most previous studies have merely focused on P adsorption on pure FeO in the lab, leading to an overestimation of the P adsorption and fixation capacities of FeO in the real environment, especially in the organic-rich agricultural areas where phosphate fertilizer is over-used. On the other hand, formation of FeO–OM complexes, as an important mechanism for the stabilization of OM, enables carbon fixation in soil, which could affect the global carbon cycle and global warming (Lalonde et al., 2012; Lützow et al., 2006). Thus, the results here can be further used to understand the eutrophication driven by P fate in the context of global climate change.

Formation of iron mineral-OM complexes in the field of P adsorption described above, which preferentially decreases P adsorption, also explains the phenomenon that P adsorption is lower in humic-rich soil/sediments although iron minerals are abundant, in contrast to mineral soils (Fontes et al., 1992). Our data show that the traditional P adsorption mechanism, established through direct adsorption on the raw mineral surfaces, does not accurately describe the true mode of P immobilization in soil/sediment, especially in high OM load areas such as wetlands, forest floors and riparian belts.

3. Conclusions

The results show that the presence of HA decreases the specific surface area of FeO, especially amorphous FeO, but did not change their internal structure. The P adsorption capacities of FeO–HA complexes were all less than those of the corresponding raw FeO. Additionally, the decrease trend for P adsorption on amorphous FH was far greater than that of crystalline GE. HA coated on FeO may affect P adsorption by competitively occupying the sites on the mineral surface or through changing electrostatic repulsion. However, the main adsorption surface could still be the iron mineral rather than HA. Meanwhile, increasing pH inhibited P adsorption, while increasing ionic strength promoted P adsorption. It is interesting that the strong dependence on ionic strength of P adsorption might demonstrate that, for P adsorption on iron mineral-OM, outer-sphere complexes between the OM component surface and P possibly coexist with inner-sphere surface complexes between the iron mineral component and P. These results suggest that most previous studies focused on the P adsorption on raw mineral or clay may overestimate the P adsorption ability of soil/sediment in the natural environment. To the best of our knowledge, this study is the first attempt to investigate P adsorption onto FeO associated with OM.

Table 3 – Comparison of the results from references on the effect of mineral-organic matter complexes on adsorption of different pollutants.

Adsorbent	Adsorbate	Results	Mechanism	Reference
Hematite-humic substance	Hydrophobic organic compounds (HOC)	HOC adsorbed increased with increasing humic substances loaded	Hydrophobicity increased	Murphy et al. (1990)
GE/hematite-HA	Phenanthrene	The binding coefficients, $K_{b(oc)}$, obtained for dissolved HA were much higher than the sorption coefficients, $K_{p(oc)}$, obtained for Mineral-HA	Less available sites	Laor et al. (1998)
FH-HA	Imidazolinone herbicides	More HA loaded on FH-HA, more herbicide adsorbed	Hydrophobicity increased	Leone et al. (2001)
Hematite-HA	Cd^{2+}	Cd^{2+} adsorption increased compared with both single component	Provided new available adsorption sites	Vermeer et al. (1999)
FH-tartrate/oxalate	Cu^{2+}, Cr^{3+}, Pb^{2+}	More carbon content on adsorbent, more heavy metals adsorbed	Provided new available adsorption sites	Zhu et al. (2010)
FH-fulvic acid	Pb^{2+}	Pb^{2+} adsorption increased compared with FH	Provided new available adsorption sites	Wei and Xiang (2013)
Hematite-HA	As(V), As(III)	A lower adsorption capacity compared with bare hematite	HA occupied the adsorption sites	Ko et al. (2004)
FH/GE/hematite-HA	As(V)	As(V) adsorption decreased compared with pure iron oxides	HA occupied the adsorption sites and the positive charge decreased	Xie (2012)
Fe^{3+}-HA	PO_4^{3-}	The molar ratio $P_{adsorbed}$/Fe of Fe^{3+}-HA complex was higher than amorphous Fe-oxide	Formed ternary complex *via* metal bridge between P and HA	Gerke and Hermann (1992)

FH: ferrihydrite; GE: goethite; HA: humic acid; FH-HA: ferrihydrite-humic acid; GE-HA: goethite-humic acid.

Acknowledgments

This work was supported by the National Natural Science Foundation of China (Nos. 41171198, 41403079), the China Postdoctoral Science Foundation (No. 2013M542238), the Chongqing Special Postdoctoral Science Foundation (No. Xm2014023), and the Fundamental Research Funds for the Central Universities (No. XDJK2015B035).

REFERENCES

Antelo, J., Avena, M., Fiol, S., López, R., Arce, F., 2005. Effects of pH and ionic strength on the adsorption of phosphate and arsenate at the goethite-water interface. J. Colloid Interface Sci. 285 (2), 476–486.

Antelo, J., Fiol, S., Pérez, C., Mariño, S., Arce, F., Gondar, D., et al., 2010. Analysis of phosphate adsorption onto ferrihydrite using the CD-MUSIC model. J. Colloid Interface Sci. 347 (1), 112–119.

Arai, Y., Sparks, D.L., 2001. ATR-FTIR spectroscopic investigation on phosphate adsorption mechanisms at the ferrihydrite-water interface. J. Colloid Interface Sci. 241 (2), 317–326.

Arai, Y., Sparks, D.L., 2007. Phosphate reaction dynamics in soils and soil components: a multiscale approach. Adv. Agron. 94, 135–179.

Axt, J.R., Walbridge, M.R., 1999. Phosphate removal capacity of palustrine forested wetlands and adjacent uplands in Virginia. Soil Sci. Soc. Am. J. 63 (4), 1019–1031.

Baldock, J.A., Skjemstad, J.O., 2000. Role of the soil matrix and minerals in protecting natural organic materials against biological attack. Org. Geochem. 31 (7-8), 697–710.

Borggaard, O.K., Raben-Lange, B., Gimsing, A.L., Strobel, B.W., 2005. Influence of humic substances on phosphate adsorption by aluminium and iron oxides. Geoderma 127 (3), 270–279.

Cruz-Guzmán, M., Celis, R., Hermosin, M.C., Leone, P., Nègre, M., Cornejo, J., 2003. Sorption–desorption of lead (II) and mercury (II) by model associations of soil colloids. Soil Sci. Soc. Am. J. 67 (5), 1378–1387.

Ekholm, P., Lehtoranta, J., 2012. Does control of soil erosion inhibit aquatic eutrophication? J. Environ. Manag. 93 (1), 140–146.

Elsner, M., Schwarzenbach, R.P., Haderlein, S.B., 2004. Reactivity of Fe (II)-bearing minerals toward reductive transformation of organic contaminants. Environ. Sci. Technol. 38 (3), 799–807.

Fontes, M.R., Weed, S.B., Bowen, L.H., 1992. Association of microcrystalline goethite and humic acid in some Oxisols from Brazil. Soil Sci. Soc. Am. J. 56 (3), 982–990.

Geelhoed, J.S., Hiemstra, T., Van Riemsdijk, W.H., 1997. Phosphate and sulfate adsorption on goethite: single anion and competitive adsorption. Geochim. Cosmochim. Acta 61 (12), 2389–2396.

Geelhoed, J.S., Hiemstra, T., Van Riemsdijk, W.H., 1998. Competitive interaction between phosphate and citrate on goethite. Environ. Sci. Technol. 32 (14), 2119–2123.

Gerke, J., Hermann, R., 1992. Adsorption of orthophosphate to humic-Fe-complexes and to amorphous Fe-oxide. Z. Pflanzenernähr. Bodenkd. 155 (3), 233–236.

Gu, B., Schmitt, J., Chen, Z., Liang, L., McCarthy, J.F., 1994. Adsorption and desorption of natural organic matter on iron oxide: mechanisms and models. Environ. Sci. Technol. 28 (1), 38–46.

Hay, M.B., Myneni, S.C.B., 2007. Structural environments of carboxyl groups in natural organic molecules from terrestrial systems. Part 1: infrared spectroscopy. Geochim. Cosmochim. Acta 71 (14), 3518–3532.
Henneberry, Y.K., Kraus, T.E.C., Nico, P.S., Horwath, W.R., 2012. Structural stability of coprecipitated natural organic matter and ferric iron under reducing conditions. Org. Geochem. 48, 81–89.
Hiemstra, T., Mia, S., Duhaut, P.B., Molleman, B., 2013. Natural and pyrogenic humic acids at goethite and natural oxide surfaces interacting with phosphate. Environ. Sci. Technol. 47 (16), 9182–9189.
Kaiser, K., Guggenberger, G., 2000. The role of DOM sorption to mineral surfaces in the preservation of organic matter in soils. Org. Geochem. 31 (7-8), 711–725.
Kaiser, K., Guggenberger, G., 2003. Mineral surfaces and soil organic matter. Eur. J. Soil Sci. 54 (2), 219–236.
Kalbitz, K., Schwesig, D., Rethemeyer, J., Matzner, E., 2005. Stabilization of dissolved organic matter by sorption to the mineral soil. Soil Biol. Biochem. 37 (7), 1319–1331.
Kleber, M., Eusterhues, K., Keiluweit, M., Mikutta, C., Mikutta, R., Nico, P.S., 2015. Mineral–organic associations: formation, properties, and relevance in soil environments. Adv. Agron. 130, 1–140.
Ko, I., Kim, J.Y., Kim, K.W., 2004. Arsenic speciation and sorption kinetics in the As-hematite-humic acid system. Colloids Surf. A 234 (1), 43–50.
Lalonde, K., Mucci, A., Ouellet, A., Gélinas, Y., 2012. Preservation of organic matter in sediments promoted by iron. Nature 483, 198–200.
Laor, Y., Farmer, W.J., Aochi, Y., Strom, P.F., 1998. Phenanthrene binding and sorption to dissolved and to mineral-associated humic acid. Water Res. 32 (6), 1923–1931.
Leone, P., Nègre, M., Gennari, M., Boero, V., Cornejo, J., 2001. Adsorption of imidazolinone herbicides on ferrihydrite-humic acid associations. J. Environ. Sci. Health B 36 (2), 127–142.
Lijklema, L., 1980. Interaction of orthophosphate with iron(III) and aluminum hydroxides. Environ. Sci. Technol. 14 (5), 537–541.
Lu, L., Gao, M., Gu, Z., Yang, S., Liu, Y., 2014. A comparative study and evaluation of sulfamethoxazole adsorption onto organo-montmorillonites. J. Environ. Sci. 26 (12), 2535–2545.
Lützow, M.V., Kögel-knabner, I., Ekschmitt, K., Matzner, E., Guggenberger, G., Marschner, B., et al., 2006. Stabilization of organic matter in temperate soils: mechanisms and their relevance under different soil conditions—a review. Eur. J. Soil Sci. 57, 426–445.
Mazzetti, L., Thistlethwaite, P.J., 2002. Raman spectra and thermal transformations of ferrihydrite and schwertmannite. J. Raman Spectrosc. 33 (2), 104–111.
Murphy, J., Riley, J.P., 1962. A modified single solution method for the determination of phosphates in natural water. Anal. Chim. Acta 27, 31–36.
Murphy, E.M., Zachara, J.M., Smith, S.C., 1990. Influence of mineral-bound humic substances on the sorption of hydrophobic organic compounds. Environ. Sci. Technol. 24 (10), 1507–1516.
Musić, S., Gotić, M., Popović, S., 1993. X-ray diffraction and Fourier transform-infrared analysis of the rust formed by corrosion of steel in aqueous solutions. J. Mater. Sci. 28 (21), 5744–5752.
Nelson, P.N., Baldock, J.A., Oades, J.M., 1992. Concentration and composition of dissolved organic carbon in streams in relation to catchment soil properties. Biogeochemistry 19 (1), 27–50.
Qin, X., Liu, F., Wang, G., Huang, G., 2015. Adsorption of humic acid from aqueous solution by hematite: effects of pH and ionic strength. Environ. Earth Sci. 73 (8), 4011–4017.
Rahnemaie, R., Hiemstra, T., van Riemsdijk, W.H., 2007. Geometry, charge distribution, and surface speciation of phosphate on goethite. Langmuir 23 (7), 3680–3689.
Russell, J.D., 1979. Infrared spectroscopy of ferrihydrite: evidence for the presence of structural hydroxyl groups. Clay Miner. 14 (2), 109–114.
Schwertmann, U., 1966. Inhibitory effect of soil organic matter on the crystallization of amorphous ferric hydroxide. Nature 212, 645–646.
Schwertmann, U., Cornell, R.M., 2000. Iron Oxides in the Laboratory: Preparation and Characterization. 2nd ed. Wiley-VCH, Weinheim, Germany.
Schwertmann, U., Wagner, F., Knicker, H., 2005. Ferrihydrite-humic associations: magnetic hyperfine interactions. Soil Sci. Soc. Am. J. 69 (4), 1009–1015.
Sharma, P., Ofner, J., Kappler, A., 2010. Formation of binary and ternary colloids and dissolved complexes of organic matter, Fe and As. Environ. Sci. Technol. 44 (12), 4479–4485.
Sharpley, A.N., Chapra, S.C., Wedepohl, R., Sims, J.T., Daniel, T.C., Reddy, K.R., 1994. Managing agricultural phosphorus for protection of surface waters, issues and options. J. Environ. Qual. 23 (3), 437–451.
Shimizu, M., Zhou, J., Schröder, C., Obst, M., Kappler, A., Borch, T., 2013. Dissimilatory reduction and transformation of ferrihydrite-humic acid coprecipitates. Environ. Sci. Technol. 47 (23), 13375–13384.
Sposito, G., 1989. The Chemistry of Soils. Oxford University Press, New York, USA, p. 277.
Stellacci, P., Liberti, L., Notarnicola, M., Bishop, P.L., 2009. Valorization of coal fly ash by mechano-chemical activation: part I. Enhancing adsorption capacity. Chem. Eng. J. 149 (1), 11–18.
Tadanier, C.J., Eick, M.J., 2002. Formulating the charge-distribution multisite surface complexation model using FITEQL. Soil Sci. Soc. Am. J. 66 (5), 1505–1517.
Vermeer, A.W.P., McCulloch, J.K., Van Riemsdijk, W.H., Koopal, L.K., 1999. Metal ion adsorption to complexes of humic acid and metal oxides: deviations from the additivity rule. Environ. Sci. Technol. 33 (21), 3892–3897.
Wang, X., Li, W., Harrington, R., Liu, F., Parise, J.B., Feng, X., et al., 2013a. Effect of ferrihydrite crystallite size on phosphate adsorption reactivity. Environ. Sci. Technol. 47 (18), 10322–10331.
Wang, X., Liu, F., Tan, W., Li, W., Feng, X., Sparks, D.L., 2013b. Characteristics of phosphate adsorption-desorption onto ferrihydrite: comparison with well-crystalline Fe (hydr) oxides. Soil Sci. 178 (1), 1–11.
Wei, F., 2002. Methods for Water and Wastewater Monitoring and Analysis. 4th ed. China Environmental Science Press, Beijing, China.
Wei, S., Xiang, W., 2013. Adsorption removal of Pb (II) from aqueous solution by fulvic acid-coated ferrihydrite. J. Food Agric. Environ. 11 (2), 1376–1380.
Wei, S., Tan, W., Liu, F., Zhao, W., Weng, L., 2014. Surface properties and phosphate adsorption of binary systems containing goethite and kaolinite. Geoderma 213, 478–484.
Weng, L., Van Riemsdijk, W.H., Koopal, L.K., Hiemstra, T., 2006a. Adsorption of humic substances on goethite: comparison between humic acids and fulvic acids. Environ. Sci. Technol. 40 (24), 7494–7500.
Weng, L., Van Riemsdijk, W.H., Koopal, L.K., Hiemstra, T., 2006b. Ligand and Charge Distribution (LCD) model for the description of fulvic acid adsorption to goethite. J. Colloid Interface Sci. 302 (2), 442–457.
Weng, L., Van Riemsdijk, W.H., Hiemstra, T., 2008. Humic nanoparticles at the oxide-water interface: interactions with phosphate ion adsorption. Environ. Sci. Technol. 42 (23), 8747–8752.

Xie, Y., 2012. Adsorption and Desorption Characteristics of Arsenate on Iron Oxides and Their Complexes With Humic Acids. Southwest University, Chongqing, China (Master Thesis).

Xiong, Y., Li, Q., 1987. China Soil. Science Press, Beijng, China, pp. 390–417.

Xu, Y., Yang, M., He, C., Xiong, H., 2013. Characterization and spectral analysis of the stable mineral phases α, β-FeOOH included in iron oxyhydroxides. Spectrosc. Spectr. Anal. 33 (12), 3330–3333.

Zhang, Y., Lin, X., Werner, W., 2003. The effect of soil flooding on the transformation of Fe-oxides and the adsorption/desorption behavior of phosphate. J. Plant Nutr. Soil Sci. 166 (1), 68–75.

Zhu, J., Pigna, M., Cozzolino, V., Caporale, A.G., Violante, A., 2010. Competitive sorption of copper(II), chromium(III) and lead(II) on ferrihydrite and two organomineral complexes. Geoderma 159 (3-4), 409–416.